Korean J. Chem. Eng., 35(2), 409-420 (2018)
DOI: 10.1007/s11814-017-0307-7

pISSN: 0256-1115
eISSN: 1975-7220

Process optimization for selective hydrogenation of α-pinene over $Ni/AlPO_4$

Chen Yang, Lihong Jiang, Huaibo Wang, Yane Zheng, and Yaming Wang†

Faculty of Chemical Engineering, Kunming University of Science and Technology, Kunming 650500, P. R. China
(*Received 13 June 2017 • accepted 5 November 2017*)

Abstract−A new supported $Ni/AlPO_4$ catalyst was synthesized and studied for the selective hydrogenation of α-pinene to prepare *cis*-pinane. The support was flaky morphology with orthorhombic phase and Ni was well dispersed. The surface area of the catalyst was 37.62 $m^2 \cdot g^{-1}$ with a pore size of 2.83 nm. For the hydrogenation reaction, the performance of the catalyst was positively correlated with the surface area of support and loading content of Ni. Effects of hydrogenation condition were determined and the process was optimized by response surface methodology. The result suggested that the conversion was positively correlated to hydrogenation temperature, duration and catalyst dosage, while the selectivity showed a negative correlation to temperature and catalyst dosage. After optimization, 95.1% of selectivity was obtained under 94.8% of conversion at 405 K, 81 min and 2.28 wt% of catalyst.

Keywords: Aluminophosphate, Nickel, Selective Hydrogenation, α-Pinene, *cis*-Pinane, Response Surface Methodology

INTRODUCTION

With the development of industrialization and increase of population, fossil resources are enduring huge consumption. For achieving the "sustainable development" and "green chemistry", efficient exploitation and effective utilization of renewable resource are now under growing attention and research. Turpentine is important renewable forest resource that is widely used in synthesis of fine chemicals, biological inhibitors and functional materials [1-3]. As the distillation product of resin, turpentine is globally distributed and can be easily obtained by collecting the resultant exudates of living pine tree [4]. Turpentine consists mainly of monoterpenes such as pinene, camphene, myrcene and small amount of monoterpene alcohols. Generally, the content of pinene is much more than others.

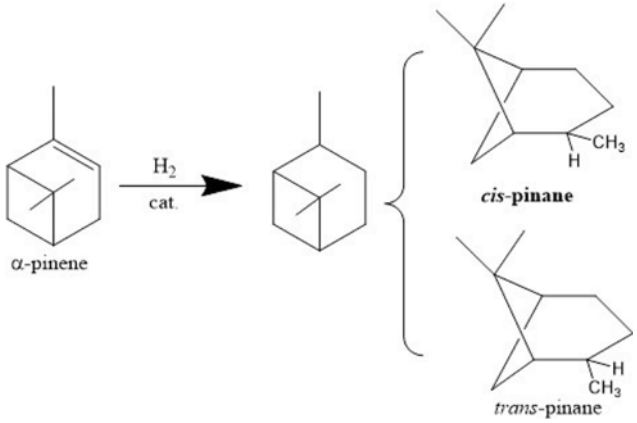

Scheme 1. Reaction equation of α-pinene hydrogenation.

Due to the various functional groups, pinene is chemically active and apt to be hydrogenated, isomerized, oxidized and polymerized, and the derivatives are widely used and applied in many fields [5-8]. Hydrogenation of α-pinene produces a mixture of *cis*-pinane and *trans*-pinane (Scheme 1). *cis*-Pinane is an important chemical intermediate that can be used for the synthesis of high value-added chemicals and specialty pharmaceuticals like linalool [1], citronellol and dihydromyrcenol; thus, increasing the selectivity of *cis*-pinane is very important for selective hydrogenation of α-pinene.

Commonly, precious metals catalysts such as Pt, Ru, Pd and nonprecious metals catalysts like Ni are used for hydrogenation of pinene. Researches on precious-metal-catalyzed reaction demonstrated that the precious metals are active for hydrogenation of α-pinene at comparatively moderate reaction conditions [9-12]. However, additional solvent is usually required [11,12] in the reaction, so the separation of the products and the recovery of the catalyst is difficult. Besides, the precious metals are expensive, which also increases the costs.

Since the early twentieth century, Ni-based catalysts have been utilized for the hydrogenation of pinene. Because nickel is cheaper than precious metals and the preparation of nickel catalysts is easier than that of precious metals, Ni-based catalysts have been more frequently studied and applied for this reaction [13-16]. Supported Ni was more researched because it has the advantages of both active center and support. Besides, it is easy to separate the solid catalyst and liquid products. Ren et al. [17,18] synthesized Ni/Al_2O_3 for continuous hydrogenation of α-pinene, and 94.5% of α-pinene converted to pinane with 74.9% of *cis*-pinane selectivity. Wang et al. [19,20] prepared Ni/SFCC catalyst for α-pinene hydrogenation, where 90.2% of selectivity of *cis*-pinane was obtained at certain condition. Our previous research [21] suggested that Ni/TiO_2-Al_2O_3 synthesized with sol-gel method showed good performance for this reaction that 92.7% of selectivity was obtained under 89.8% of conversion. These researches revealed the good catalytic property

†To whom correspondence should be addressed.
E-mail: wym@kmust.edu.cn

of Ni-based catalysts for conversion of pinene, while the selectivity of *cis*-pinane was not considerable. Since different hydrogenation performance was presented utilizing the same active center in above researches, it was supposed that a proper support might be benefit to obtaining superior selectivity.

Aluminophosphate molecular sieves [22] are good catalyst supports for many reactions [23,24] because of their large surface area with microporous or mesoporous structure. Furthermore, aluminophosphates possess electrically neutral framework, so they have excellent thermal stability, hydrothermal stability, are free of catalytic property and oxidation resistance. Because of these properties, side reactions can be avoided when aluminophosphates are used as catalyst support [25,26]. Since first being successfully synthesized in 1982 [22], researches on aluminophosphates were frequently reported [27-29]. Solvothermal method was often used in synthesis of aluminophosphate where alcohols, liquid alkanes and ionic liquids were used as solvent [30,31], while the usage of turpentine, a common solvent for many other researches [32-34], was not reported yet.

There has been no specific report about the preparation of Ni/$AlPO_4$ and the utilization in hydrogenation of biomass resources, or the synthesis of $AlPO_4$ via solvothermal method with pinene as solvent. We designed this Ni/$AlPO_4$ catalyst for the hydrogenation of α-pinene to obtain *cis*-pinane. Supports and catalysts were characterized by XRD, N_2-sorption, SEM, TEM, TG-DSC, H_2-TPR and O_2-TPO. According to the previous studies, many factors affected the hydrogenation reaction; thus effects of hydrogenation factors were investigated by single factor experiment. Furthermore, the process was optimized by response surface methodology. The results suggested that this catalytic system had several advantages. The synthesis method was environmentally friendly and economical, and the catalyst showed excellent activity for reaction and was effectively recycled.

EXPERIMENT

1. Synthesis of Support and Catalysts

The support $AlPO_4$ was synthesized by solvothermal synthesis. Aluminum hydroxide ($Al(OH)_3$, AR), ortho-phosphoric acid (H_3PO_4, AR), triethanolamine ($(HOCH_2CH_2)_3N$, AR, noted as "R") and pinene (IP, noted as "Sol") acted as Al source, P source, template and solvent, respectively. A typical synthesis procedure of $AlPO_4$ was as follows: Reactants were mixed at the mole ratio of 1Al : 1P : 1R : 60Sol; the mixture was placed to hydrothermal reactor for crystallization at 453 K for 24 h; the crystallization product was calcined in muffle at 823 K for 5 h to remove template. The obtained support was labelled as Su-#.

A typical loading procedure was as follows: 1 g support was impregnated into 10 mL nickel nitrates ($Ni(NO_3)_2{\cdot}6H_2O$) solution where nickel ion's concentration was 10 wt% under ultrasonic vibration for 1 h. Then the solvent was evaporated under infrared lamp and the remaining solid powder ($Ni(NO_3)_2/AlPO_4$) was calcined at 723 K for 3 h in muffle. After calcination, the catalyst precursor $NiO/AlPO_4$ was prepared. Before the hydrogenation reaction, the catalyst was activated by H_2 at 723 K for 2 h in tubular muffle. A typical obtained catalyst was labelled as Ni(*x*wt%)/Su-#, where the *x* presented the nickel ion's concentration in the nickel nitrates solution and the Su-# meant the entry of support.

2. Catalysts Characterization

The phase of catalysts was identified by X-Ray diffraction (XRD) on Rigaku D/max-2200 with Cu Kα radiation (λ=0.15406 nm). The operating voltage and current were 40 kV and 200 mA. The scanning rate was $5^{o}{\cdot}min^{-1}$.

The morphological and microstructural attributes of catalysts were observed by scanning electron microscope (SEM) on Tescon Vega3 (U=5 kV) with Octane Prime Det EDX detector (EDS) and transmission electron microscope (TEM) on FEI Tecnai G2 20 (U=200 kV).

The specific surface area and pore volume of the supports were determined by nitrogen adsorption-desorption at 77 K on Quantachrome Nova 4200e. BET method and BJH model were used for the calculation and analysis of certain data. In the following text, the BET specific surface area was abbreviated as "BET".

The thermal properties of catalysts were analyzed by thermal gravimetric analysis with differential scanning calorimetry (TG-DSC) on Netzsch STA-449 F3 and temperature-programmed reduction/oxidation (H_2-TPR/O_2-TPO) on Quantachrome ChemBet 3000. The heating rate was 10 $K{\cdot}min^{-1}$ for the three tests in all. For TPR test, the pretreated sample was exposed to 10% H_2/Ar (80 $mL{\cdot}min^{-1}$) up to 873 K. For TPO test, the pretreated sample was exposed to 10% O_2/N_2 (80 $mL{\cdot}min^{-1}$) up to 973 K.

3. Catalytic Activity for Hydrogenation

The catalytic activity of prepared catalyst was tested by hydrogenation of α-pinene. A typical hydrogenation procedure was as follows: 10 g α-pinene, 0.3 g catalyst (noted as 3 wt%) and the rotor were put into the autoclave with magnetic stirring, then the reactor was sealed and purged repeatedly with nitrogen and hydrogen to eliminate air. 4 MPa of hydrogen was charged into the autoclave for reaction. The reaction was performed at 403 K for 60 min with stirring speed of 800 rpm.

Reactant and hydrogenated products were analyzed in a gas chromatograph (Fisons, GC8340) with SE-30 capillary column and FID. The performance of catalysts for hydrogenation was evaluated by the conversion of α-pinene and the selectivity of *cis*-pinane, the main hydrogenated product.

4. Optimization of Process

The hydrogenation reaction was optimized with single factor experiment (SFE) and response surface methodology (RSM). The effects of main conditions including hydrogenation temperature, catalyst dosage and hydrogenation duration on the reaction were investigated by SFE, and the optimal condition was determined by RSM. For RSM, Design-Expert® (Version 8.0.6) was used to design the experiments and analyze the data.

RESULTS AND DISCUSSION

1. Characterization of $AlPO_4$ and Ni/$AlPO_4$

1-1. Structure and Surface Properties of Catalysts

XRD patterns of the support and catalyst in four stages are shown in Fig. 1(A). Pattern (a) suggests that the $AlPO_4$ (PDF#48-0652) was obtained, and the formation of this phase was due to the reaction of Al and P with AlO(OH) [35]. A prominent peak (2θ=20.5°)

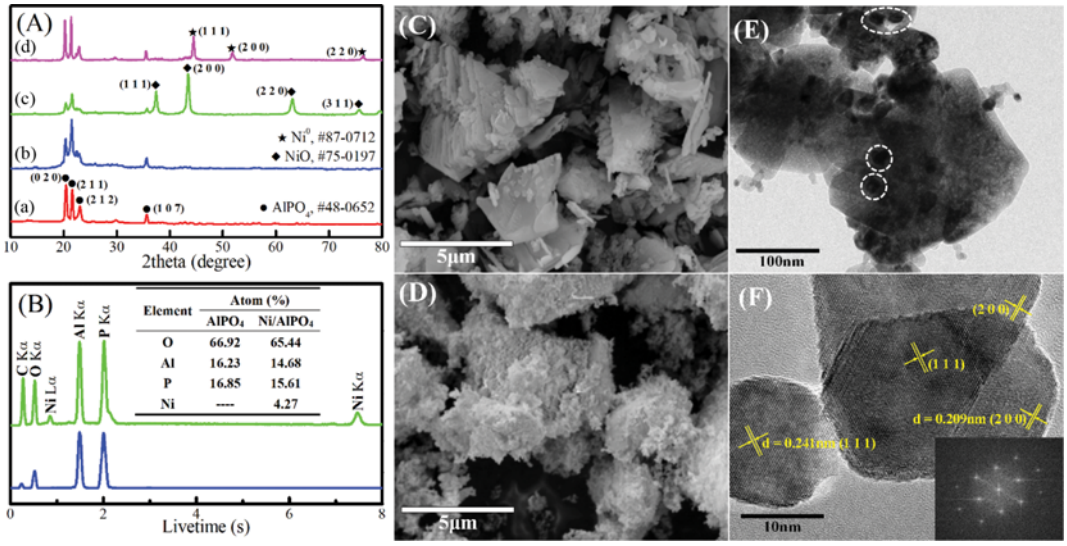

Fig. 1. The phase and Microstructure of a certain catalyst. XRD patterns (A) of support as-synthesized (a), support calcined (b), catalyst precursor (c) and catalyst activated (d). SEM images of support $AlPO_4$ (C) and catalyst precursor $NiO/AlPO_4$ (D) with EDS patterns (B), and TEM (E) and HRTEM images (F) of $NiO/AlPO_4$.

corresponding to (0 2 0) reflection followed by peaks at 21.6°, 23.1° and 35.7° corresponding to (2 1 1), (2 1 2) and (1 0 7) reflection, respectively. After calcination, the main phase of support was not changed, while the intensity of (0 2 0) plane weakened (Pattern (b)), which indicated that calcination changed partial crystalline of $AlPO_4$ and caused partial structure collapse [36]. Some weaker peaks observed at 2θ=12.9°, 14.9° and 22.4°, etc. corresponding to AFI phase reflection indicated that a small amount of APO-5 was synthesized [37]. The phases of both NiO (PDF#75-0197) and $AlPO_4$ could be observed in Pattern (c), and the addition of NiO made the peaks of the $AlPO_4$ weakened. Pattern (d) revealed that Ni^0 (PDF#87-0712) was obtained after the reduction of NiO. It suggested that the activation procedure did not change the formation of support. After reduction, the oxygen atom from NiO that covered the support surface outflowed and gave rise to the strengthening of the peaks of $AlPO_4$ again. A particularly weak peak observed at 2θ=43.5° was possibly due to inevitable oxidation of Ni.

SEM and TEM images of catalyst are also shown in Fig. 1. It was observed from Fig. 1(C) that the support mainly had a flaky morphology, while some flaks reunited. Fig. 1(D) shows the morphology of catalyst precursor that active ingredient (NiO) was well-dispersed on the surface of $AlPO_4$, and the loading procedure did not change the morphology of support. TEM image of catalyst precursor shown on Fig. 1(E) suggests that NiO had dispersed on the support and the presence was confirmed by the dark field [38], which was consistent with the SEM results. The deeper dark area in the figure demonstrated that NiO was stacked [39] in that region as noted in the image. From Fig. 1(F), the HRTEM image of catalyst precursor, the lattice fringes of NiO are clearly observed, and the planes can be identified as (1 1 1) and (2 0 0) planes. Besides, the dark area verifies the stack of NiO, which is consistent with Fig. 1(E).

The elemental composition of support and catalyst precursor were identified by energy-dispersive X-ray spectroscopy (EDS, Fig.

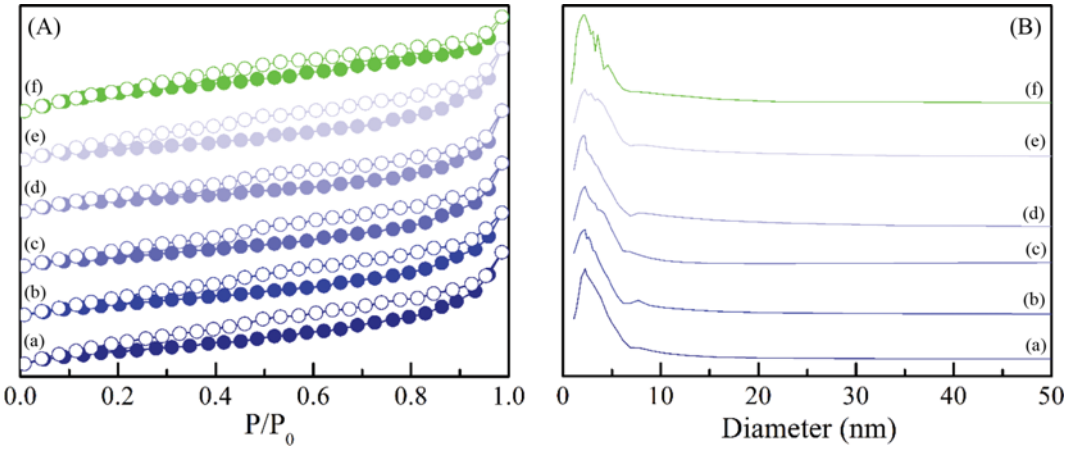

Fig. 2. Nitrogen adsorption-desorption isotherms (A) and the pore distribution (B) of different samples.

Table 1. Surface properties of different supports and catalyst

Entry	Sample	Crystallization duration (h)	Crystallization temperature (K)	S_{BET} ($m^2 \cdot g^{-1}$)	Average pore size (nm)	Pore volume ($\times 10^{-2}$ $cm^3 \cdot g^{-1}$)
a	Su-1	28	433	115.83	2.81	10.45
b	Su-2	28	453	110.70	2.68	9.68
c	Su-3	28	473	92.44	3.17	9.52
d	Su-4	20	433	128.66	2.52	10.52
e	Su-5	36	433	103.52	3.14	10.46
f	Ni(10 wt%)/Su-4	--	--	37.62	2.83	5.43

1(B)). Chemical characterization of the typical sample showed that the support was composed of oxygen, phosphate and aluminum by the molar ratio of ca. 1Al : 1.04P : 4.12O, ie.1 : 1 : 4. The catalyst precursor was confirmed to be composed of nickel, oxygen, aluminum and phosphate. According to the atom percentage, about 4.3 mol NiO was loaded on 15 mol $AlPO_4$, and it could be calculated that the concentration of Ni was about 2.18 $mmol \cdot g^{-1}$ Ni : $AlPO_4$.

N_2 adsorption-desorption isotherms of the samples are shown in Fig. 2(A). The isotherms of the support samples (a)-(e) all obey the IV type (definition by IUPAC), which is characteristic of mesoporous materials [40], and this result was confirmed by the pore size distribution shown in Fig. 2(B) as well. The same type of the isotherms was obtained, which suggested that the pore structure type was not affected by crystallization temperature or duration. Su-4 and Ni(10 wt%)/Su-4 showed the same type of isotherms ((d) and (f)), which indicated that the loading procedure had no obvious effect on the pore structure of support.

The data of surface properties of different samples are displayed in Table 1. It was observed that crystallization temperature affected the specific surface area, pore distribution and pore volume of $AlPO_4$s. When crystallization duration lasted for 28 h, the BET of $AlPO_4$ at 433 K was 115.83 $m^2 \cdot g^{-1}$. Raising the temperature to 453 and 473 K, the BET declined to 110.7 and 92.44 $m^2 \cdot g^{-1}$, respectively, which indicated that a higher crystallization temperature might make the BET smaller. Crystallization duration also had effect on the surface properties. At 20 h of duration, the BET reached 128.66 $m^2 \cdot g^{-1}$, while it continuously decreased to 103.52 $m^2 \cdot g^{-1}$ at 36 h. This phenomenon suggests that longer crystallization duration might cause the BET smaller. Pore structure was not obviously affected by crystallization condition. The average pore size of support ranged from 2.5 to 3.2 nm, and the change of pore volume was less than

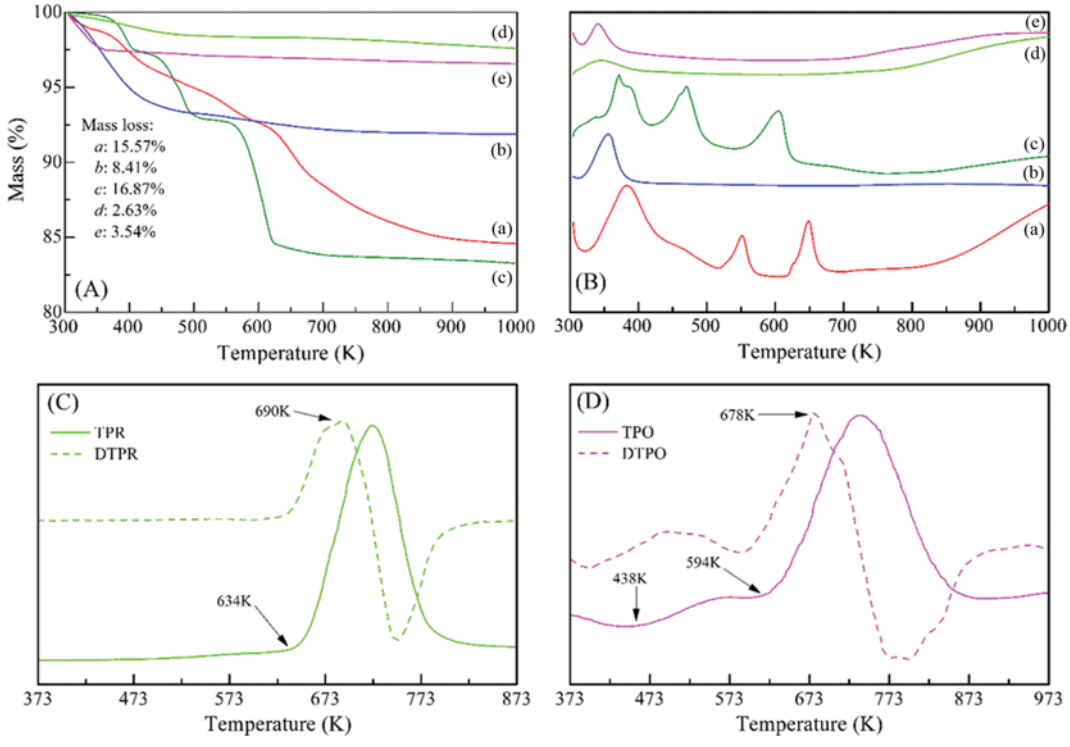

Fig. 3. TG (A) and DSC (B) curves of $AlPO_4$ as-synthesized ((a), *test in air*), $AlPO_4$ calcined ((b), *test in air*), $Ni(NO_3)_2/AlPO_4$ ((c), *test in air*), $NiO/AlPO_4$ ((d), *test in air*) and $Ni/AlPO_4$ ((e), *test in nitrogen*), and the H_2-TPR test (C) of $NiO/AlPO_4$ and O_2-TPO test (D) of $Ni/AlPO_4$.

0.01 $mL \cdot g^{-1}$. In addition, the variation trend of pore size agreed with that of BET, yet the pore volume did not show the consistency. Entry (f) demonstrated that Ni occupied part of channel and surface of support after loading and led to the decline of BET and pore volume.

1-2. Thermal Properties of Catalysts

TG analysis of support (Su-4) and catalyst (Ni(10 wt%)/Su-4) in different stages was investigated (Fig. 3(A)). For the curve (a), four stages of weight loss were observed. The first two stages from 323 to 440 K were assigned to the desorption of water, where the former one from 323 to 383 K corresponded to the volatilization of free water, and the latter one from 393 to 440 K corresponded to the desorption of bound water. The amount of weight loss in these stages indicated that the water in the as-synthesized sample was about 4.10 wt%. The weight losses from 540 to 900 K were assigned to the decomposition of triethanolamine [41,42], in which the loss from 620 to 700 K corresponded to the breaking down of N-C bond [41]. Above 700 K, the curve becomes smooth, which indicates that the procedure of template removal was steady. When the temperature reached 900 K, the weight almost remained constant, indicating that the triethanolamine was totally removed. 11.96% of the mass was reduced in this stage, which suggested that the template occupied about 11.96 wt% in the as-synthesized sample. For curve (c), three weight losses stages were observed. The weight loss from 363 to 433 K was due to the desorption of bound water. No obvious loss was observed before 373 K, which evidenced that little free water existed in the $Ni(NO_3)_2/AlPO_4$, and the content of bound water was about 2.51 wt%. The weight losses from 440 to 510 K and 560 to 620 K were ascribed to the oxidation of nickel nitrate, where the former one corresponded to the formation of Ni_2O_3 and the latter one represented the formation of NiO [43]. For this sample, 14.36% of mass was reduced. Only one stage of weight loss was observed in curves (b), (d) and (e), respectively, which was ascribed to the volatilization of free water and evidenced that the certain samples had excellent thermal stability. For the three samples, the weight losses were only caused by free water, so the values of weight losses indirectly reflected the pore volumes of the samples. The amount of weight loss of (b) (8.41%) was more than that of (d) (2.63%) and (e) (3.54%), which was ascribed that the active center occupied part of the surface and channel of the support after loading and led to a decline of pore volume (see Table 1).

DSC curves of the samples are shown in Fig. 3(B). For curve (a), three peaks are observed. Associated with the TG curve, the first peak corresponds to the desorption of water and the following ones are due to the decomposition of triethanolamine. For curve (c), three peaks are observed and they are assigned to the desorption of water and the conversion of $Ni(NO_3)_2$. Only one peak is seen in curves (b), (d) and (e), respectively, which corresponds mainly to the desorption of free water. The result evidences that the support and catalyst are thermally stable. The intensity of the three peaks could be ranged by (b)>(e)>(d), which is positively correlated to the mass loss. Furthermore, the endothermic peaks corresponding to water in sample (a) and (e) emerged later than in other three samples, which indicates that the desorption temperature of water in the two samples was higher than in other three samples. This phenomenon demonstrates that the as-synthesized $AlPO_4$ and $Ni(NO_3)_2/AlPO_4$ mainly contain bound water, while another three samples only contain free water.

H_2-TPR curves of catalyst precursor $NiO/AlPO_4$ and O_2-TPO curves of activated catalyst $Ni/AlPO_4$ are shown in Fig. 3(C) and Fig. 3(D). TPR test described a typical reduction procedure of NiO. The TPR curve reveals that the reduction starts at about 634 K and ends at 813 K with a maximum reducing amount at 723 K, which is consistent with the reference that the reduction of supported Ni often starts from 690 K [44]. The DTPR curve shows that the reduction maximizes at 690 K, indicating that this catalyst was more active and more likely to be activated. TPO test describes a typical oxidation procedure of Ni and the curve shows an obvious two-stair oxidation procedure. The former one beginning at 438 K corresponds to the oxidation of shattered or stacked Ni and the latter one beginning at 594 K corresponds to the major oxidation of catalyst. DTPO curve shows that the oxidation was maximized at 678 K, which demonstrates that the major inactivation of catalyst might take place at that temperature. The result also indicated that the catalyst was stable at room conditions and fit to the reaction.

2. Catalytic Property for Hydrogenation of α-Pinene

The synthesized aluminophosphates were supported by Ni and used for the hydrogenation of α-pinene. The hydrogenation result

Table 2. Catalytic performance, surface area and loading of catalysts

Entry	Catalyst	S_{BET} ($m^2 \cdot g^{-1}$)		Concentration of Ni[b] ($mmol \cdot g^{-1}$ Ni : $AlPO_4$)	Conversion (%)	Selectivity (%)
		Support	Catalyst[a]			
1	Ni(10 wt%)/Su-1	115.83	36.67	2.11	90.9	94.8
2	Ni(10 wt%)/Su-2	110.70	30.58	2.13	87.9	92.3
3	Ni(10 wt%)/Su-3	92.44	43.73	1.88	72.0	91.1
4	Ni(10 wt%)/Su-4	128.66	37.62	2.18	94.2	95.0
5	Ni(10 wt%)/Su-5	103.52	39.12	2.05	83.8	91.2
6	Ni(5 wt%)/Su-4	128.66	61.73	1.31	44.0	95.5
7(4)	Ni(10 wt%)/Su-4	128.66	37.62	2.18	94.2	95.0
8	Ni(15 wt%)/Su-4	128.66	23.69	3.27	98.3	90.5

[a]The N_2-sorption isotherms and pore size of catalysts were shown in Fig. S2

[b]The concentration of Ni in the catalyst was calculated from EDS data that shown in Fig. S1 and Table S1

and characterization of catalysts are shown in Table 2.

In the presence of Ni/$AlPO_4$ catalysts, the hydrogenation of α-pinene occurred well in that the selectivity of *cis*-pinane was more than 90%.

Su-1~Su-5 were, respectively, impregnated into $Ni(NO_3)_2$ solutions with the same concentration of nickel ion (10 wt%), and the hydrogenation result and the characterization of catalysts are displayed in Entry 1-5. When using the solution with same concentration of nickel ion (10 wt%), the loading of Ni in catalysts ranged from 1.88 to 2.23 mmol·g^{-1} Ni : $AlPO_4$. Generally, the support with larger BET could support more nickel, while the sequence of loading amount was not consistent with the BET of support. After Ni loading, the BET of the catalyst obviously decreased. For the five catalysts, the BET ranged from 31.58 to 43.73 $m^2 \cdot g^{-1}$, and the sequence was not consistent with the BET of support.

The conversion of pinene went from 72.0% to 94.3%, and the selectivity of *cis*-pinane ranged from 91.1% to 95.0%. The two sets of data showed the same order: Ni(10 wt%)/Su-4>Ni(10 wt%)/Su-1>Ni(10 wt%)/Su-2>Ni(10 wt%)/Su-5>Ni(10 wt%)/Su-3, and this sequence was consistent with the BET of support. It could be supposed that for the five catalysts, the one with larger BET of support might have better performance. According to the BET and EDS data, there was no obvious correlation between the catalytic performance and the BET of catalyst or the content of Ni. Associated with the synthesis condition of support, the catalyst with the support synthesized at lower crystallization temperature and shorter crystallization duration showed better performance.

Entries 6-8 showed a correlation between the catalytic performance and the loading of Ni, where Su-4 was selected as support and impregnated into $Ni(NO_3)_2$ solutions with various concentration of nickel ion (5 wt%-15 wt%). At the nickel ion's concentration of 5 wt%, 10 wt% and 15 wt% in the $Ni(NO_3)_2$ solution, the actual loadings of Ni were 1.31, 2.18 and 3.27 mmol·g^{-1} Ni : $AlPO_4$, and the BET of catalysts were 61.73, 37.62 and 23.69 $m^2 \cdot g^{-1}$, respectively. The result revealed that more nickel could load on the support when larger concentration of nickel ion was present in the solution. Meanwhile, when more Ni was loaded on the support, the BET of catalyst got smaller because more part of support was occupied. When the loading of Ni ranged from 1.31 to 3.27 mmol, the conversion increased from 44.0% to 98.3% while the selectivity decreased from 95.5% to 90.5%. Therefore, a higher concentration of Ni might lead to an increase of conversion and declining of selectivity.

The phenomenon that larger BET of support and less loading of Ni made the selectivity higher could be explained by the possible reaction mechanism reported by other researchers. The research suggested that the surface reaction of the adsorbed H and pinene on the catalyst was the rate-controlling step [19] as well as the steric hindrance to the adsorption on a catalyst surface [45]. The support with larger BET could provide larger contact surface to reduce the steric hindrance, which was in favor to the formation of *cis*-pinane. However, when more active ingredient is loaded on the support, the steric hindrance might occur during the surface reaction and lead to the formation of *trans*-pinane.

Furthermore, the conversion or selectivity did not show consistency with the content of Ni in the catalyst when different supports were used, while they showed monotonic trend with the content of Ni when using the same support. This phenomenon evidenced that the BET of support plays an important role for the certain reaction when the Ni/$AlPO_4$ catalyst is used.

Table 3. Comparison of catalytic performances and surface properties of different supported Ni catalysts

Catalyst*	S_{BET} of support ($m^2 \cdot g^{-1}$)	Conversion (%)	Selectivity (%)
Ni/Su-4[a]	128.66	94.2	95.0
Ni/APO-5[b]	276.90	89.1	89.7
Ni/4A[c]	300.15	84.1	90.1

*Loading procedure followed section 2.1, and provided in supplementary data

[a]Ni(10wt%)/Su-4

[b]Synthesis procedure of APO-5 was shown in supplementary data

[c]Commercial catalyst support

To facilitate comparison, two kinds of catalysts were prepared (Table 3). Under the same hydrogenation condition, the conversion and selectivity over the Ni(10 wt%)/Su-4 were 94.3% and 95.0%, much better than that over Ni/APO-5 (89.1%/89.7%) or Ni/4A (84.1%/90.1%), even if the BET of Su-4 was far smaller than that of APO-5 or 4A. Particularly, Su-4 was prepared with similar method as APO-5, except the solvent replacement into water, and the BET being less than half, while the selectivity was enhanced by 5%. Compared with Ni/SFCC [19] and Ni/TiO_2-Al_2O_3 [21], 7% of exaltation of conversion was obtained over Ni(10 wt%)/Su-4 where selectivity was increased by about 5%. Besides, the loading of Ni and the catalyst dosage in this catalytic system were both less than in the two. These facts indicate that the supported catalyst with same active center, whose support was prepared with solvent of pinene, could show better catalytic activity for hydrogenation of α-pinene.

3. Optimization of Hydrogenation Reaction

In this section, the effect of hydrogenation condition was investigated by SFE and the process was optimized by RSM. According to the result shown in Table 2, the catalyst Ni(10 wt%)/Su-4 showed better activity for the reaction than the other catalysts. Thus, this catalyst was used for the optimization of hydrogenation reaction.

3-1. Effect of Conditions on the Reaction

The effects of hydrogenation temperature from 383 to 423 K, hydrogenation duration from 30 to 150 min, and catalyst dosage from 1 wt% to 9 wt% were investigated and the results are illustrated in Fig. 4. It was observed from Fig. 4(a) that the temperature had a strong effect on the reaction. A significant leap of conversion appeared from 18.2% (383 K) to 99.2% (423 K), and underwent an obvious gradient between 383 and 403 K, which reveals that a higher temperature could promote the conversion of α-pinene. The selectivity was only 88.2% at 383 K while leaping to 94.3% at 393 K, which indicates that the catalyst could not well exert its activity at low temperature. The selectivity continuously decreased with the increase of temperature from 393 to 423 K, which suggests that higher temperature might cause the formation of *trans*-pinane. This phenomenon was ascribed to the fact that the α-pinene and hydrogen molecules motioned strenuously and more easily con-

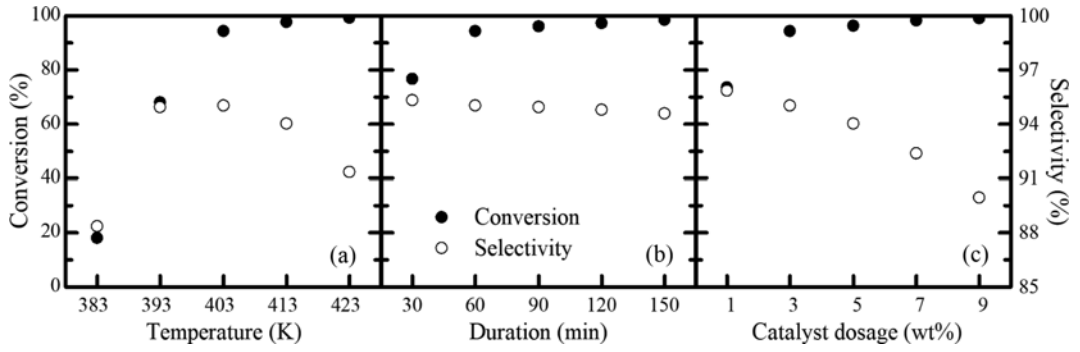

Fig. 4. Effect of reaction condition on the hydrogenation of α-pinene. Reaction conditions: Reactants: 10 g α-pinene and 4 MPa H_2 in a 50 mL autoclave; Duration investigated: 403 K/3 wt%; Temperature investigated: 60 min/3 wt%; Catalyst dosage investigated: 60 min/ 403 K.

tacted on the catalyst at high temperature. Since the surface reaction was the rate-controlling step, the over rapid contact might give rise to the occurrence of steric hindrance on the surface of catalyst in the formation of *cis*-pinane and make the α-pinene convert to *trans*-pinane.

The effect of hydrogenation duration is shown in Fig. 4(b). The conversion reaches 76.5% after 30 min and leaps to 94.2% after 60 min, then increases mildly to 98.5% after 150 min, which suggests that this catalyst has excellent activity, and could cause a considerable conversion at short duration. The selectivity shows a small decline from 95.3% to 94.6% with the prolonging of duration, which indicates that when the reaction steadily proceeds, *cis*-pinane and *trans*-pinane could be produced at a generally stable ratio.

Fig. 4(c) shows the effect of catalyst dosage on the reaction. Conversion was positively correlated to catalyst dosage while selectivity showed a negative correlation. Conversion increased from 73.6% to 99.1% with the catalyst dosage added from 1 wt% to 9wt%, which shows that conversion is significantly affected by catalyst dosage. Selectivity decreases monotonically from 95.7% to 89.8% with the increasing of catalyst dosage, indicating that overdose of catalyst is unfavorable to the selectivity. According to the mechanism, when overdose catalyst was used, large amount of reactants gathered on the surface of catalyst, which led to the occurrence of severe steric hindrance in the formation of *cis*-pinane and made the α-pinene convert to *trans*-pinane. Besides, the possibility of shifting the reaction to the diffusion-controlled region existed if overdose of catalyst was added [14].

3-2. RSM Optimizing of Process

Since the conversion and selectivity showed generally opposite correlation with hydrogenation conditions, an optimizing test was designed to determine the proper condition. RSM is a useful and common method for process optimization [46,47]; thus it was

Table 4. Experimental matrix of RSM Box-Behnken Design and experimental result

Run	Variables			Response		
	A: Temperature (K)	B: Duration (min)	C: Cata-dosage (wt%)	Conversion (%)	Selectivity (%)	Yield (%)
1	393	120	3	80.3	94.4	75.7
2	403	90	3	95.4	94.7	90.4
3	403	60	5	94.9	94.5	89.6
4	413	90	5	98.5	93.4	92.0
5	403	60	1	77.6	96.2	74.6
6	403	90	3	96.6	94.8	91.6
7	413	60	3	96.8	94.1	91.1
8	403	90	3	95.8	94.6	90.6
9	403	120	5	98.3	94.2	92.6
10	403	90	3	95.9	94.7	90.8
11	413	90	1	88.6	94.4	83.7
12	393	90	1	66.7	96.2	64.2
13	393	90	5	74.5	93.6	69.8
14	403	90	3	95.4	94.8	90.5
15	413	120	3	97.6	93.1	90.9
16	393	60	3	64.1	94.6	60.6
17	403	120	1	78.1	95.8	74.8

used here and Box-Behnken Design (BBD) was used to investigate the effect of operating parameters. Usually, for the selective hydrogenation reaction, selectivity is more important than conversion; thus the selectivity and a new target, Yield, the product of conversion and selectivity, were selected as the functions. The levels of factors were picked as follows: 393, 403 and 413 K for temperature (A); 60, 90 and 120 min for duration (B); 1 wt%, 3 wt% and 5 wt% for catalyst dosage (C). The experiment matrix and result are shown in Table 4. After the evaluation of experimental results, quadratic functions for the selectivity and yield were obtained. The function of conversion is shown but not for analysis.

$$\text{Con}(\%) = -14076.59760 + 67.79369A + 5.79890B + 0.08020C - 0.01278AB + 0.02654AC + 0.01203BC - 0.08129A^2 - 3.32774\times10^{-3}B^2 - 1.40205C^2$$

$$\text{Sel}(\%) = -1048.71708 + 5.73885A + 0.23835B - 8.64245C - 6.34750\times10^{-4}AB + 0.01880AC + 4.43081\times10^{-4}BC - 7.17875\times10^{-3}A^2 + 4.53996\times10^{-5}B^2 + 0.09815C^2$$

$$\text{Yield}(\%) = -14382.26719 + 69.44558A + 5.74394B - 4.30108C - 0.01275AB + 0.03406AC + 0.01145BC - 0.08351A^2 - 3.13598\times10^{-3}B^2 - 1.25758C^2$$

Table 5 displays the result of analysis of variance (ANOVA) for the responses of selectivity and yield, which demonstrated the significance and fitness of the model as well as the effects of significant individual terms and their interactions on the chosen responses [48,49]. The F value is a statistically reliable evaluation of how well the factors explain the change in the data about its mean and can be estimated from ANOVA [50], and the "Prob>F" values indicate the significance of each term in the ANOVA [51]. For the two responses, values of "Prob>F" less than 0.05 indicate that model terms are significant and that greater than 0.10 indicates the model terms are not significant.

For the selectivity, there was only a 0.01% chance that a "Model F-Value" this large could occur due to noise. The main effects of temperature (A), duration (B) and catalyst dosage (C), the second-order effects of temperature (A^2) and catalyst dosage (C^2), interaction effects of temperature with duration (AB) and catalyst dosage with temperature (AC) were significant and emerged as the major determinant, while the second-order effects of duration (B^2) and interaction effects of duration with catalyst dosage (BC) were insignificant and less affected in the studied range, which was consistent with the SFE result that catalyst dosage and temperature showed stronger effect on the selectivity.

The perturbation plot for the selectivity is shown in Fig. 5(A1). The plot demonstrates the effects of all factors at a central point in the design space. It indicates that the duration had insignificant effect on the selectivity, yet the catalyst dosage and temperature had significant effects, and the selectivity was negatively correlated to the catalyst dosage as well as the temperature. This result agreed with that in SFE as well.

A comparison of the experimental values with the predicted values of selectivity from the above equation is depicted in Fig. 5(B1). The result demonstrates an excellent convergence between the

Table 5. Analysis of variance (ANOVA) for the two responses

Source	Sum of square	DF	Mean square	F-value	Prob>f
Selectivity					
A	1.84	1	1.84	104.83	<0.0001
B	0.46	1	0.46	25.93	0.0014
C	6.18	1	6.18	351.68	<0.0001
AB	0.15	1	0.15	8.26	0.0239
AC	0.57	1	0.57	32.19	0.0008
BC	2.827×10^{-3}	1	2.827×10^{-3}	0.16	0.7002
A^2	2.17	1	2.17	123.56	<0.0001
B^2	7.030×10^{-3}	1	7.030×10^{-3}	0.40	0.5470
C^2	0.65	1	0.65	36.95	0.0005
Residual	0.12	7	0.018		
	R^2=0.9898, Adj-R^2=0.9766, Pred-R^2=0.8806, Adequate precision=31.120				
Yield					
A	953.60	1	953.60	102.79	<0.0001
B	40.81	1	40.81	4.40	0.0742
C	270.84	1	270.84	29.19	0.0010
AB	58.53	1	58.53	6.31	0.0403
AC	1.86	1	1.86	0.20	0.6682
BC	1.89	1	1.89	0.20	0.6655
A^2	293.63	1	293.63	31.65	0.0008
B^2	33.54	1	33.54	3.62	0.0990
C^2	106.54	1	106.54	11.48	0.0116
Residual	64.94	7	9.28		
	R^2=0.9652, Adj-R^2=0.9205, Pred-R^2=0.4500, Adequate precision=14.329				

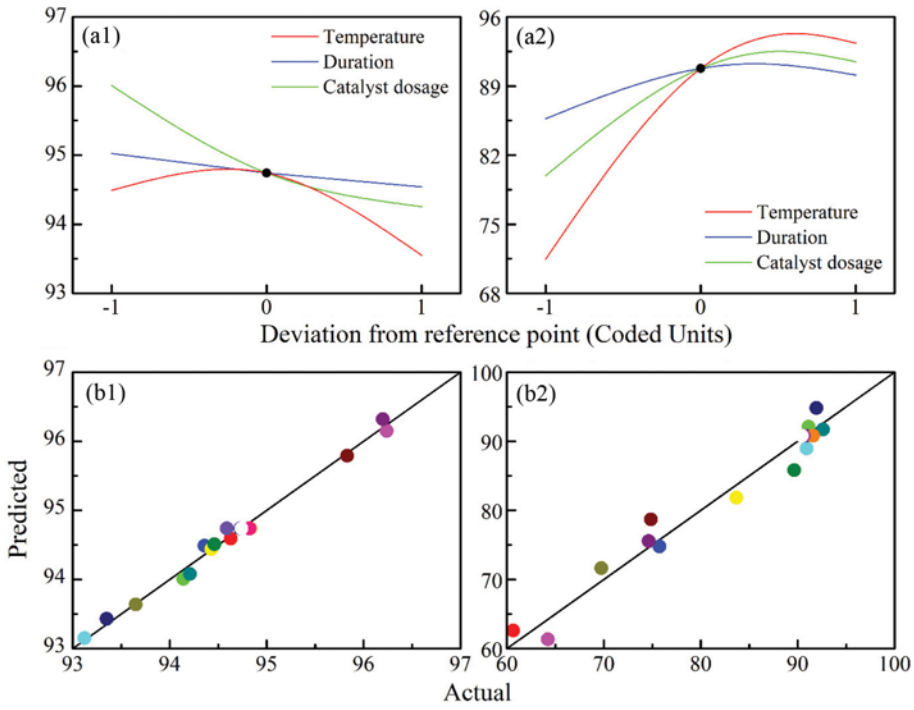

Fig. 5. Perturbation (a) and PvA (b) plot of selectivity (1) and yield (2).

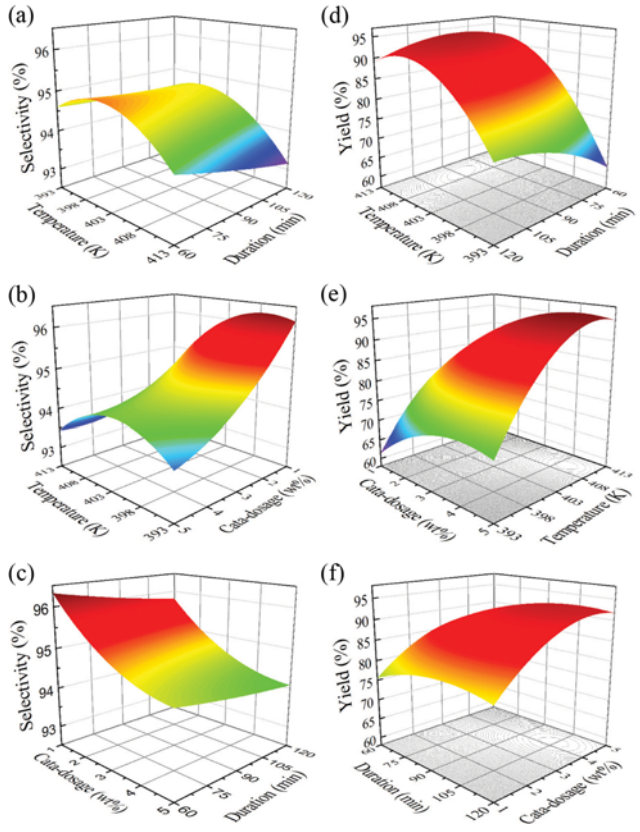

Fig. 6. Response surface plot for the interaction effects of the process variables on selectivity (a)-(c) and yield (d)-(f). (a) & (d): temperature and duration at 3 wt% of catalyst dosage; (b) & (e): catalyst dosage and temperature at 90 min of duration; (c) & (f): duration and catalyst dosage at 403 K of temperature.

experimental and simulated values (R^2=0.9766).

The interaction effects of the process parameters on selectivity are illustrated by three-dimensional response surface curves. These curves were plotted on the basis of the empirical model and shown in Fig. 6(a)-(c).

Fig. 6(a) shows the joint effect of temperature and duration on the selectivity. With the enhancement of temperature, the effect of duration became increasingly prominent, and a prolonging of duration led to an obvious decline of selectivity. The selectivity-temperature curves kept the arched shape at any duration values in the studied range where the selectivity was higher at lower temperature, which indicates that the proper temperature for the selectivity was lower than 403 K. The joint effect of catalyst dosage and temperature on the selectivity is shown in Fig. 6(b). A monotonic decreasing of selectivity emerged with larger catalyst dosage particularly at lower temperature. The effect of temperature showed the arched shape like Fig. 6(a). With the increasing dosage of catalyst, the effect of temperature weakened and the proper value was verified from 396 to 403 K. The joint effect of duration and catalyst dosage on the selectivity is shown in Fig. 6(c). With the decreasing dosage of catalyst, the effect of duration was increasingly substantial. A prolonging of duration caused an obvious decline of selectivity, just in contrast with the joint effect of temperature-duration. The same trend was observed in the effect of catalyst dosage.

The yield was calculated from the product of conversion and selectivity. Although it was an indirect result, its importance was doubtless because it reflected the purity of pinane product. Thus, it meant the target of this process of obtaining "a high selectivity of *cis*-pinane under considerable conversion of α-pinene."

For the yield, there was only a 0.03% chance that a "Model F-

Value" this large could occur due to noise. In this case, the main effects of temperature (A) and catalyst dosage (C), the second-order effects of temperature (A^2) and catalyst dosage (C^2), and the interaction effects of temperature with duration (AB) were significant and emerged as the major determinant, while the interaction effects of duration with catalyst dosage (BC) and catalyst dosage with temperature (AC) were insignificant and less affected in the studied range. The result revealed that the yield was mainly affected by the conversion, which was because the conversion was more sensitive to reaction condition. In addition, this trend was also consistent with the SFE.

An interesting phenomenon was observed: Although the temperature (A) and catalyst dosage (C) were significant, their interaction (AC) was insignificant. This might be because the conversion reached a high level (96.0%) at the initial level stage (403 K/90 min/3 wt%), which made it difficult to be raised. Run 4 showed that when the factors were both at the upper level, the conversion was 98.5%, only 2.5% of ascent. But when they were both at the lower level (Run 12), conversion was only 66.7%, verifying the significance of the factors. Another possibility could be supposed from Run 11 and Run 13 that the effect of temperature was far stronger than catalyst dosage, which made the effect of catalyst dosage or interaction "unobvious". That is, compared with the temperature, the catalyst dosage or interaction between catalyst dosage and temperature was "insignificant."

The perturbation plot for the yield is shown in Fig. 5(A2). The plot demonstrates the effects of all factors at a central point in the design space. Yield was positively correlated to all factors when they were before half-upper level (0.5 as coded units), then it became negative. This variation could be interpreted as the opposite trends of conversion and selectivity. Before ca. half-upper level, the increasing of conversion was far more significant than the decreasing of selectivity; thus, conversion acted as the major factor and gave rise to a conspicuous increasing of yield. After half-upper level, the conversion flattened, while the selectivity decreased more rapidly, which led to the decreasing of yield.

A comparison of the experimental values with the predicted values of yield from the above equation is given in Fig. 5(B2). The result demonstrates a good convergence between the experimental and simulated values (R^2=0.9205).

The interaction effects of the process parameters on yield are graphically illustrated by three-dimensional response surface curves. These curves were plotted on the basis of the empirical model and shown in Fig. 6(d)-(f).

Fig. 6(d) shows the joint effect of temperature and duration on the yield. The effect of temperature was manifest in all duration range especially at low levels. The yield kept increasing with temperature at short duration, but at long duration, yield decreased with enhancement of the temperature. The yield was obviously affected by the duration and showed a positive correlation at low temperatures. At high temperature, the effect of duration weakened, while the yield sustained at high levels. An obvious decline of yield occurred at high levels of both, suggesting that it was not conducive to the production of *cis*-pinane at over-strong condition. The joint effect of catalyst dosage and temperature on the yield is shown in Fig. 6(e). The result reveals that the significance of both factors could be attributed to their strong effects to the conversion, as presented before. A small decline of yield took place at the upper level for both, which was similar to temperature-duration surface and could be explained by the influence of the relative significance between conversion and selectivity. Fig. 6(f) shows the joint effect of duration and catalyst dosage. It was observed that the effect and interaction of these two factors were mild. The yield increased steadily and then decreased with the increasing of catalyst dosage in all duration range. The effect of duration on the yield was slight.

To determine the optimum conditions for the pinene hydrogenation process, a numerical optimization method in the Design Expert software was utilized. In this case, all factors were selected within the range. The ranges of the reaction temperature, duration and catalyst dosage were 393-413 K, 60-120 min and 1 wt%-5 wt%. The goal for this process was to enhance the yield while keeping selectivity as high as possible. Therefore, the selectivity was set to be upper than 95.0% at normal importance, and the yield was set to be maximum at high importance, respectively. Based on this target, the optimum process variables were obtained at the values by temperature of 405.38 K, duration of 81.19 min and catalyst dosage of 2.28 wt%, which was selected from several optimum conditions suggested by the program. Under this condition, selectivity and yield were predicted to be 95.0098% and 89.5476% with 0.939 of desirability.

A verification experiment was performed to confirm the model provided by BBD. Limited by the precision of the reactor, the actual condition of the verification experiment was at 405 K and 81 min. Three independent tests were carried out and the result is shown in Table 6. For the selectivity values, the difference between predicted and actual ones was less than ±0.1%, while actual conversion increased by 0.4% or more than predicted. It might be at-

Table 6. Predicted and actual results at predicted optimum point

Entry	Variables			Result		
	Temperature (K)	Duration (min)	Cata-dosage (wt%)	Conversion (%)	Selectivity (%)	Yield (%)
Predicted	405.38	81.19	2.28	94.2	95.0	89.5
Adj-predicted	405	81	2.28	93.9	95.0	89.2
Actual 1	405	81	2.28	94.6	95.1	89.9
Actual 2	405	81	2.28	95.0	95.1	90.4
Actual 3	405	81	2.28	94.7	95.0	90.0
Average	405	81	2.28	94.8	95.1	90.1

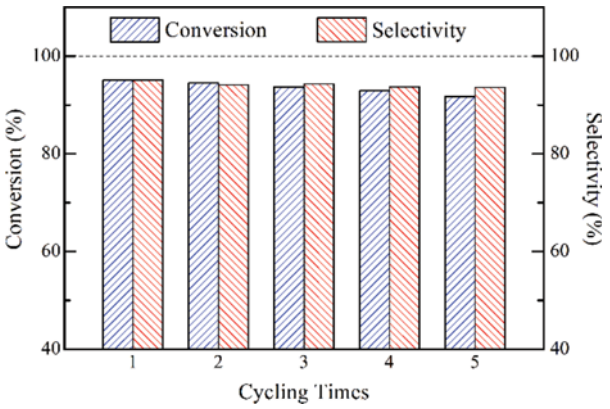

Fig. 7. Recycling performance of $Ni/AlPO_4$ for catalytic hydrogenation of α-pinene. Reaction conditions: 10 g α-pinene, 4 MPa H_2 and 0.228 g catalyst in a 50 mL autoclave at 405 K for 81 min.

tributed to some external factors. For instance, minutes ahead or delay might turn out in heating duration for reaching the target temperature. Anyway, it was gratifying that better hydrogenation result was obtained than the predicted one.

4. Reusability of Catalyst

The above experiment revealed that $Ni/AlPO_4$ could act as a good catalyst for hydrogenation of α-pinene. As a heterogeneous catalyst, its reusability was worthwhile probing. Herein, the catalyst was separated by centrifugation, and then washed, dried under nitrogen and reduced by hydrogen for a second run. As illustrated in Fig. 7, the catalyst showed an excellent activity during five times, where conversion showed a monotonic but unobvious decreasing from 94.8% to 91.8%. Selectivity also showed a slight decreasing from 95.1% to 93.5%. This result suggested that this supported catalyst had a good reusability for hydrogenation.

CONCLUSION

$AlPO_4$ was successfully synthesized by solvothermal method using pinene as solvent. The support $AlPO_4$ had a flaky morphology with orthorhombic phase. The BET surface area of support (Su-4) and catalyst (Ni(10 wt%)/Su-4) were 128.66 and 37.62 $m^2 \cdot g^{-1}$, respectively. The catalyst was efficient for the hydrogenation of α-pinene to obtain *cis*-pinane with considerable selectivity (95.1%) and high conversion (94.8%), which was better than other Ni supported catalysts. Furthermore, it was found that the surface area of support and concentration of Ni in the catalyst affected the property of catalyst. For hydrogenation conditions, the conversion was positively correlated to the temperature, duration and catalyst dosage, while the selectivity showed a negative correlation to the temperature and catalyst dosage. The catalyst also maintained good catalytic activity after successive cycle reaction. In general, this supported catalyst performed well for hydrogenation of α-pinene and worth being investigated more.

ACKNOWLEDGEMENT

We acknowledge the funds received from the National Natural Science Foundation of China (No. 21266012 and No. 21706108). We also acknowledge the support received from the Analysis and Testing Foundation of Kunming University of Science and Technology (No. 20150380).

SUPPORTING INFORMATION

Additional information as noted in the text. This information is available via the Internet at http://www.springer.com/chemistry/journal/11814.

REFERENCES

1. V. A. Semikolenov, I. I. Ilyna and I. L. Simakova, *Appl. Catal. A-Gen.*, **211**, 91 (2001).
2. P. R. Wilderman, M. B.Shah, H.-H. Jang, C. D. Stout and J. R. Halpert, *J. Am. Chem. Soc.*, **135**, 10433 (2013).
3. E. Aydin, H. Türkez and F. Geyikoğlu, *Biologia*, **68**, 1004 (2013).
4. S. Rezzi, A. Bighelli, V. Castola and J. Casanova, *Ind. Crop. Prod.*, **21**, 71 (2005).
5. D. Chouchi, D. Gourgouillon, M. Courel, J. Vital and M. Nunes da Ponte, *Ind. Eng. Chem. Res.*, **40**, 2551 (2001).
6. N. A. Comelli, E. N. Ponzi and M. I. Ponzi, *Chem. Eng. J.*, **117**, 93 (2006).
7. B. Sundaravel, C. M. Babu, R. Vinodh, W. S. Cha and H.-T. Jang, *J. Taiwan. Inst. Chem. Eng.*, **63**, 157 (2016).
8. N. A. Kukhta, I. Vasilenko and S. V. Kostjuk, *Green Chem.*, **13**, 2362 (2011).
9. S. Hou, C. Xie, F. Yu, B. Yuan and S. Yu, *RSC Adv.*, **6**, 54806 (2016).
10. S. Hou, X. Wang, C. Huang, C. Xie and S. Yu, *Catal. Lett.*, **146**, 580 (2016).
11. I. L. Simakova, Y. Solkina, I. Deliy, J. Wärnå and D. Y. Murzin, *Appl. Catal. A-Gen.*, **356**, 216 (2009).
12. X. Yang, S. Liu, C. Xie, S. Yu and F. Liu, *Chin. J. Catal.*, **32**, 643 (2011).
13. L. A. Canova, US Patent, 4,018,842 (1977).
14. S. H. Ko and T. C. Chou, *Ind. Eng. Chem. Res.*, **32**, 1579 (1993).
15. S. H. Ko, T. C. Chou and T. J. Yang, *Ind. Eng. Chem. Res.*, **34**, 457 (1995).
16. J. H. Zhang, L. H. Jiang, S. S. Wu, H. Q. Wang and Y. M. Wang, *CIESC J.*, **67**, 2363 (2016).
17. S. B. Ren, J. H. Qiu, C. Y. Wang, B. L. Xu, Y. N. Fan and Y. Chen, *Chin. J. Inorg. Chem.*, **23**, 1021 (2007).
18. S. B. Ren, J. H. Qiu, C. Y. Wang, B. L. Xu, Y. N. Fan and Y. Chen, *Chin. J. Catal.*, **28**, 651 (2007).
19. L. Wang, H. Guo, X. Chen, Y. Huang, L. Ren and S. Ding, *Can. J. Chem. Eng.*, **93**, 1770 (2015).
20. L. Wang, H. Guo, X. Chen, Y. Huang and P. Zhang, *React. Kinet. Mech. Cat.*, **114**, 639 (2015).
21. H. Han, L. H. Jiang, Y. M. Wang, T. Y. Huang and H. Q. Wang, *Chem. Ind. Fore. Prod.*, **36**, 92 (2016).
22. S. T. Wilson, B. M. Lok, C. A. Messina, T. R. Cannan and E. M. Flanigen, *J. Am. Chem. Soc.*, **104**, 1146 (1982).
23. X. Wang, F. Wang, S. Jiang and S. H. Zhong, *Chin. J. Catal.*, **32**, 352 (2011).
24. D. Chakrabortty, J. Ganguli and C. Satyanarayana, *Micropor. Meso-*

por. Mater., **137**, 65 (2011).
25. W. L. Dai, W. B. Kong, G. J. Wu, N. Li, L. D. Li and N. J. Guan, *Catal. Commun.*, **12**, 535 (2011).
26. Y. J. Lee, Y. W. Kim, N. Viswanadham, K. W. Jun and J. W. Bae, *Appl. Catal. A-Gen.*, **374**, 18 (2010).
27. S. Bhattacharjee, Y. R. Lee and W. S. Ahn, *Korean J. Chem. Eng.*, **34**, 701 (2017).
28. Z. Liu, T. Wakihara, D. Nishioka, K. Oshima, T. Takewaki and T. Okubo, *Chem. Commun.*, **50**, 2526 (2014).
29. K. Li, Z. Tian, X. Li, R. Xu, Y. Xu, L. Wang, H. Ma, B. Wang and L. Lin, *Angew. Chem. Int. Ed.*, **51**, 4397 (2012).
30. J. A. Delgado, V. I. Águeda, M. A. Uguina, J. L. Sotelo and P. Fernández, *Adsorption*, **19**, 407 (2013).
31. X. W. Song, Y. Li, L. Gan, Z. P. Wang, J. H. Yu and R. R. Xu, *Angew. Chem. Int. Ed.*, **48**, 314 (2009).
32. X. Shan, H. P. Maw and C. W. Lu, *Microsyst. Technol.*, **16**, 1501 (2010).
33. W. Xu, L. Huo, S. Luo, X. Zhang, J. Zhao, Y. Hao and Z. Ma, *Int. J. Microstruc. Mat. Prop.*, **10**, 296 (2015).
34. G. Pereira, A. Lachenwitzer, D. Munoz-Paniagua, M. Kasrai, P. R. Norton, M. Abrecht and P. Gilbert, *Tribol. Lett.*, **23**, 109 (2006).
35. K. Tang, J. Yu, Y. Zhao, Y. Liu, X. Wang and R. Xu, *J. Mat. Chem.*, **16**, 1741 (2006).
36. Y. Wang, Y. Li, Y. Yan, J. Xu, B. Guan, Q. Wang, J. Li and J. Yu, *Chem. Commun.*, **49**, 9006 (2013).
37. J. S. Chen, W. Q. Pang and R. R. Xu, *Top. Catal.*, **9**, 93 (1999).
38. E. Golubina, E. Lokteva, A. Erokhin, A. Veligzhanin, Y. V. Zubavichus, V. Likholobov and V. Lunin, *J. Catal.*, **344**, 90 (2016).
39. J. Xia, G. He, L. Zhang, X. Sun and X. Wang, *Appl. Catal. B-Environ.*, **180**, 408 (2016).
40. M. Khalfaoui, S. Knani, M. A. Hachicha and A. B. Lamine, *J. Colloid Interface Sci.*, **263**, 350 (2003).
41. Y. Liu and L. Gao, *J. Am. Ceram. Soc.*, **86**, 1651 (2003).
42. S. F. Wright, D. Dollimore, J. G. Dunn and K. Alexander, *Thermochim. Acta*, **421**, 25 (2004).
43. Y. Zhang, W. Chu, W. Cao, C. Luo, X. Wen and K. Zhou, *Plasma. Chem. Plasma. P.*, **20**, 137 (2000).
44. B. W. Hoffer, A. D. van Langeveld, J. P. Janssens, R. L. Bonné, C. M. Lok and J. A. Moulijn, *J. Catal.*, **192**, 432 (2000).
45. E. Salminen, P. Mäki-Arvela, P. Virtanen, T. Salmi and J. P. Mikkola, *Top. Catal.*, **57**, 1533 (2014).
46. A. K. Singh and M. Mukhopadhyay, *Korean J. Chem. Eng.*, **33**, 1247 (2016).
47. P. Davoodi, S. M. Ghoreishi and A. Hedayati, *Korean J. Chem. Eng.*, **34**, 854 (2017).
48. J. Cao, Y. Wu, Y. Jin, P. Yilihan and W. Huang, *J. Taiwan. Inst. Chem. Eng.*, **45**, 860 (2014).
49. O. U. Ahmed, F. S. Mjalli, T. Al-Wahaibi, Y. Al-Wahaibi and I. M. AlNashef, *Ind. Eng. Chem. Res.*, **54**, 6540 (2015).
50. A. Khataee, A. Karimi, R. D. C. Soltani, M. Safarpour, Y. Hanifehpour and S. W. Joo, *Appl. Catal. A-Gen.*, **488**, 160 (2014).
51. M. Smidt, H. Kusic, D. Juretic, M. N. Stankov, S. Ukic, T. Bolanca, M. Rogosic and A. L. Bozic, *Ind. Eng. Chem. Res.*, **54**, 5427 (2015).

Supporting Information

Process optimization for selective hydrogenation of α-pinene over Ni/$AlPO_4$

Chen Yang, Lihong Jiang, Huaibo Wang, Yane Zheng, and Yaming Wang†

Faculty of Chemical Engineering, Kunming University of Science and Technology, Kunming 650500, P. R. China
(*Received 13 June 2017 • accepted 5 November 2017*)

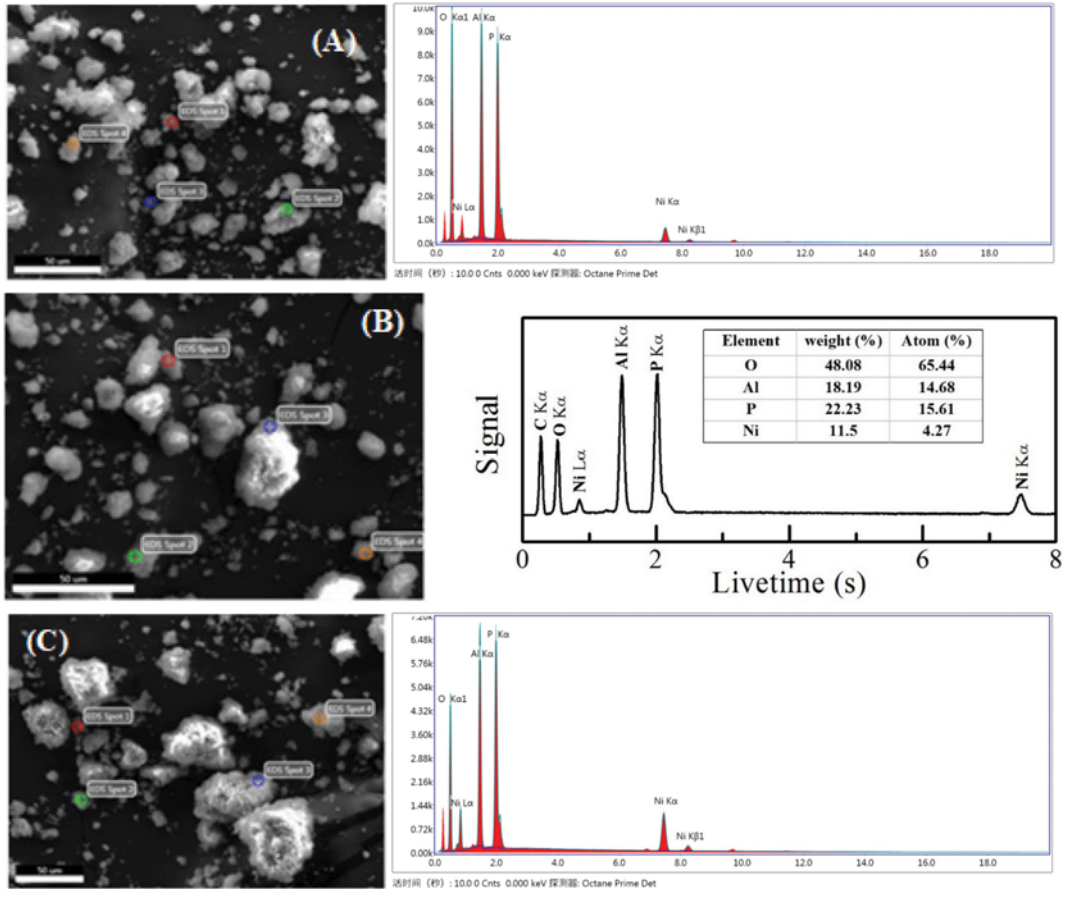

Fig. S1-1. EDS patterns of Ni(5 wt%)/Su-4 (A), Ni(10 wt%)/Su-4 (B) and Ni(15 wt%)/Su-4 (C).

1. EDS patterns of Ni(*x*wt%)/Su-#

1-1. EDS Patterns of Ni(*x*wt%)/Su-4

Su-4 was selected as the support and impregnated into $Ni(NO_3)_2$ solutions with different concentration of nickel ion (5 wt%, 10 wt% and 15 wt%), and the obtained catalysts were labelled as Ni(5 wt%)/Su-4, Ni(10 wt%)/Su-4 and Ni(15 wt%)/Su-4, respectively.

1-2. EDS Patterns of Ni(10 wt%)/Su-#

Su-1~Su-5 were respectively impregnated into $Ni(NO_3)_2$ solutions with the same concentration of nickel ion (10 wt%), and the obtained catalysts were labelled as Ni(10 wt%)/Su-1, Ni(10 wt%)/Su-2, Ni(10 wt%)/Su-3, Ni(10 wt%)/Su-4 and Ni(10 wt%)/Su-5, respectively. Since the analysis of Ni(10 wt%)/Su-4 was shown in Fig. S1-1 and Table S1-1, it was not included in the following figure or table.

2. N_2-sorption Isotherms and Pore Size of Ni(*x*wt%)/Su-#

2-1. N_2-sorption Isotherms and Pore Size of Ni(*x*wt%)/Su-4

Su-4 was selected as the support and impregnated into $Ni(NO_3)_2$ solutions with different concentration of nickel ion (5 wt%, 10 wt% and 15 wt%), and the obtained catalysts were labelled as Ni(5 wt%)/Su-4, Ni(10 wt%)/Su-4 and Ni(15 wt%)/Su-4, respectively.

2-2. N_2-sorption Isotherms and Pore Size of Ni(10wt%)/Su-#

Su-1~Su-5 were respectively impregnated into $Ni(NO_3)_2$ solutions with the same concentration of nickel ion (10 wt%), and the obtained catalysts were labelled as Ni(10 wt%)/Su-1, Ni(10 wt%)/Su-2, Ni(10 wt%)/Su-3, Ni(10 wt%)/Su-4 and Ni(10 wt%)/Su-5, respectively.

Table S1-1. Weight and molar ratio of element in the certain samples

Sample	Element	Weight (%)	Atom (%)
A Ni(5 wt%)/Su-4	O	49.24	65.72
	Al	19.86	15.71
	P	22.57	15.55
	Ni	8.33	3.02
B Ni(10 wt%)/Su-4	O	48.08	65.44
	Al	18.19	14.68
	P	22.23	15.61
	Ni	11.50	4.27
C Ni(15 wt%)/Su-4	O	45.12	64.27
	Al	16.50	13.92
	P	20.01	14.71
	Ni	18.37	7.10

Table S1-2. Weight and molar ratio of element in the certain samples

Sample	Element	Weight (%)	Atom (%)
A Ni(10 wt%)/Su-1	O	48.19	65.35
	Al	18.80	15.11
	P	22.27	15.59
	Ni	10.74	3.95
B Ni(10 wt%)/Su-2	O	48.14	65.34
	Al	18.64	14.99
	P	22.38	15.68
	Ni	10.84	3.99
C Ni(10 wt%)/Su-3	O	48.65	65.48
	Al	19.85	15.83
	P	21.78	15.13
	Ni	9.73	3.55
D Ni(10 wt%)/Su-5	O	48.26	65.38
	Al	18.47	14.83
	P	22.79	15.94
	Ni	10.48	3.85

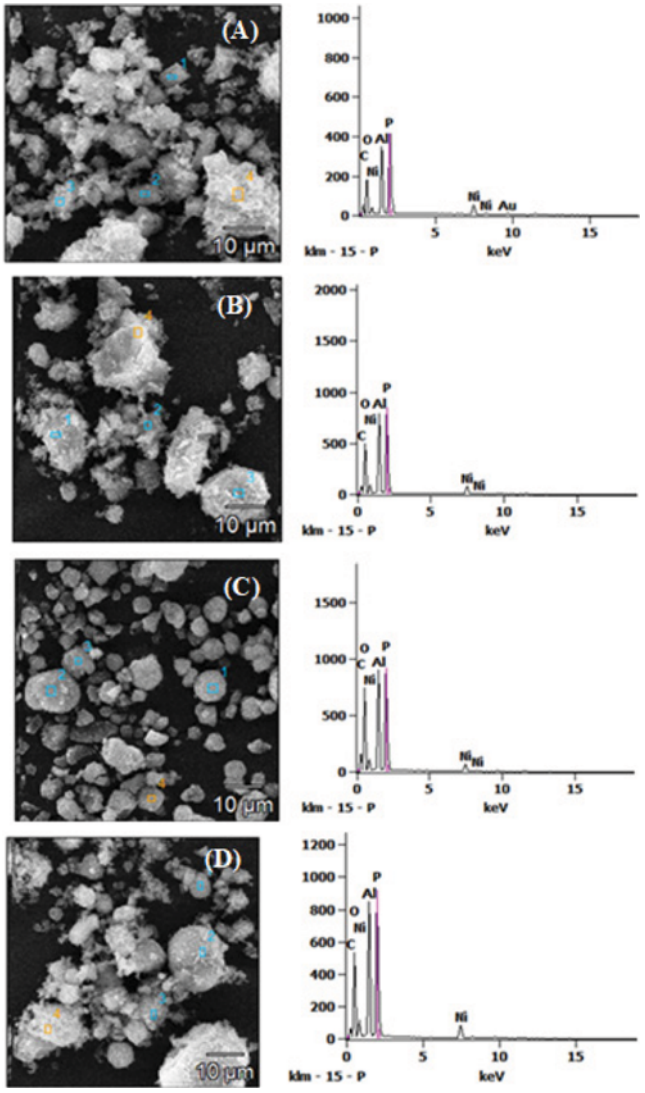

Fig. S1-2. EDS patterns of Ni(10 wt%)/Su-1(A), Ni(10 wt%)/Su-2(B), Ni(10 wt%)/Su-3(C) and Ni(10 wt%)/Su-5(D).

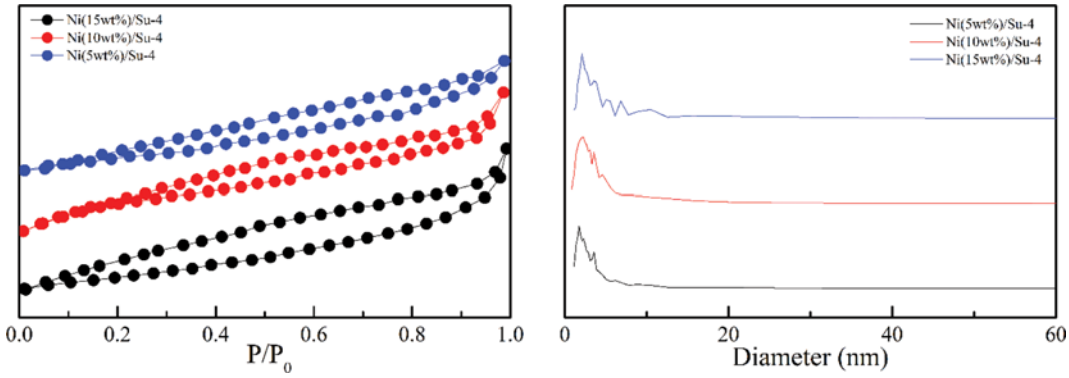

Fig. S2-1. N_2-sorption isotherms and pore size of Ni(*x*wt%)/Su-4.

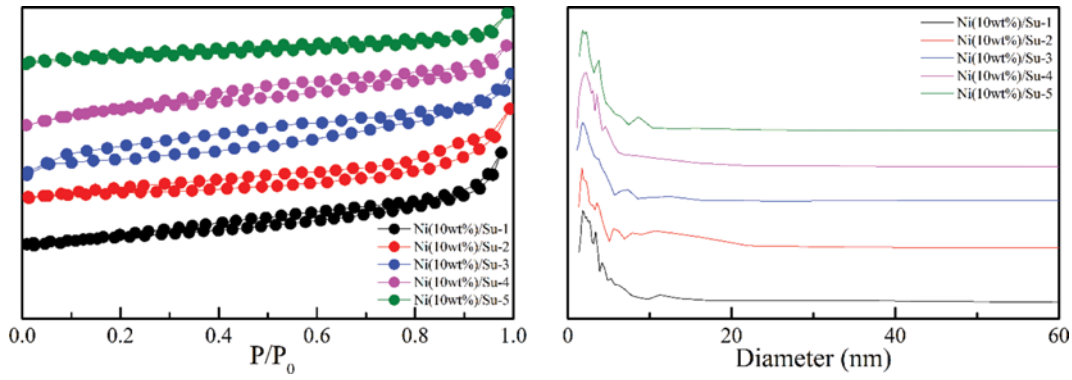

Fig. S2-2. N_2-sorption isotherms and pore size of Ni(10 wt%)/Su-#.

3. The Synthesis Condition of APO-5 (Table 3 for Section 3.2)

The support APO-5 was synthesized by hydrothermal synthesis method. Aluminum hydroxide ($Al(OH)_3$, AR), ortho-phosphoric acid (H_3PO_4, AR), Triethylamine ($(CH_3CH_2)_3N$, AR, noted as "R") and distilled water (noted as "Sol") played as Al source, P source, template and solvent, respectively. The synthesis procedure was as follow: Reactants were mixed at the mole ratio of 1Al : 1P : 1R : 60Sol; the mixture was placed to hydrothermal reactor for crystallization at 453 K for 24 h; the crystallization product was calcined in muffle at 823 K for 5 h to remove template.

4. The Loading Condition for the Catalysts in Table 3.

1 g support was impregnated into 10 mL nickel nitrates ($Ni(NO_3)_2 \cdot 6H_2O$) solution where nickel ion's concentration was 10 wt% under ultrasonic vibration for 1 h. Then the solvent was evaporated under infrared lamp and the remained solid powder was calcinated at 723 K for 3 h in muffle. After calcination, the catalyst precursor was prepared. Before the hydrogenation reaction, the catalyst was activated by H_2 at 723 K for 2 h in tubular muffle.

Table S2. The entry of the compared catalysts in Table 3

Support	Solid powder	Catalyst
Su-4	$Ni(NO_3)_2$/Su-4	Ni(10 wt%)/Su-4
APO-5	$Ni(NO_3)_2$/APO-5	Ni(10 wt%)/APO-5
4A	$Ni(NO_3)_2$/4A	Ni(10 wt%)/4A